

4.1 Introduction

Previously developed artificial gills are classified into two types: one is for portable use such as scuba diving (portable-type artificial gill), and the other is for supplying oxygen to an underwater closed-space, such as submerged vessel (plant-type artificial gill).

The portable-type artificial gill is designed to feed expired air to the membrane module [1-6]. Oxygen was transferred from water to expired air through a gas permeable membrane by oxygen partial pressure difference between water and expired air as a driving force. On the contrary, the plant-type artificial gill is designed to feed the air of the closed space to inlet a membrane module. The oxygen transfer rate of plant-type artificial gill is the lower than that of the portable type. This is because a difference in oxygen partial pressure between seawater and air in plant type is smaller than that of the portable type. In addition, the oxygen partial pressure in the air in the closed space should be lowered for increasing oxygen transfer, and human in the closed space should use low concentration of oxygen for respiration [1,4,6]. Thus, the oxygen transfer rate should be enhanced and high concentration (partial pressure of oxygen) should be provided for practical use. In chapter 3, the compact artificial gill was developed by using hemoglobin solution containing IHP. This artificial gill enhances oxygen transfer and provides high partial pressure of oxygen to respiratory air. This artificial gill would be applicable to plant-type artificial gill.

In the present chapter, a plant-type artificial gill using the concentrated hemoglobin solution, which was developed in chapter 2, was developed. The oxygen uptake rate and the oxygen release rate were estimated with the enhancement factor of the oxygen carrier solution, which was determined in chapter 3. The required heat transfer rate was also estimated to consider device

Chapter 4

efficiency of plant-type artificial gill. Optimum operating condition was determined with them, and the required device volume and energy for effectively operating device were predicted.

4.2 Experimental and Theoretical section

4.2.1 Guidelines for designing plant-type artificial gill

An artificial gill using oxygen carrier solution is consisted of four devices, oxygen uptake device from water to oxygen carrier solution, oxygen release device from oxygen carrier solution to air, device for circulating oxygen carrier solution and heat exchanger. Fig. 4.1 shows a schematic diagram of artificial gill device for supplying oxygen to underwater closed space. In this device, the concentrated hemoglobin solution was used as an oxygen carrier solution. The oxygen affinity of hemoglobin was optimized for oxygen carrier solution by adding inositol hexaphosphate (IHP). Table 4.1 shows the condition of hemoglobin solution. In the oxygen uptake device, seawater and oxygen carrier solution were made to flow outside and inside hollow fibers, respectively. Oxygen carrier solution was cooled to 293 K using seawater, and oxygen affinity of hemoglobin was increased for effective oxygen uptake. On the other hand, in the oxygen release device, oxygen carrier solution and air were made to flow outside and inside hollow fibers, respectively. Oxygen carrier solution was heated to 310 K using the heat exchanger, and oxygen affinity of hemoglobin was decreased for effective oxygen release. The oxygen partial pressure in the closed space was maintained at 20 kPa for sufficient human respiration. The oxygen consumption rate of a human in the closed space was 0.223 mmol/s, and oxygen uptake and release rates were also 0.223 mmol/s. The oxygen partial pressures of seawater were set to be 20.0 kPa and 12.0 kPa for ordinary and deficient oxygen condition in water, respectively [7-8].

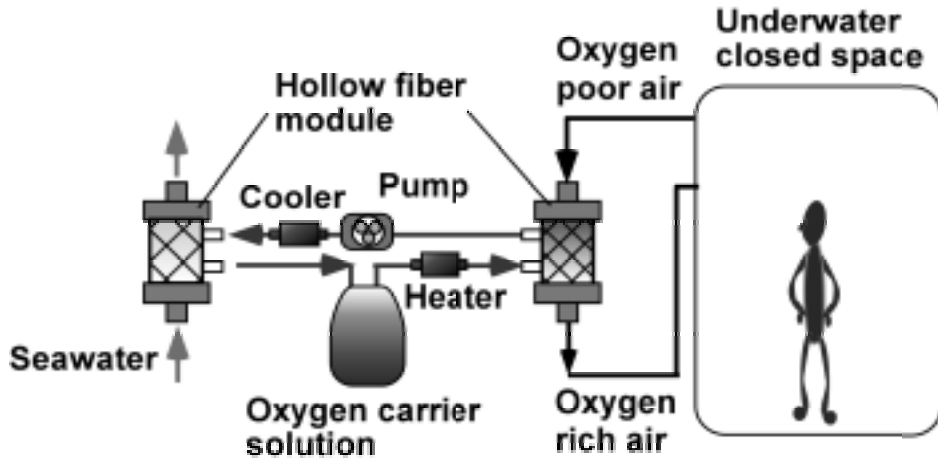


Figure 4.1 Schematic diagram of artificial gill for supplying oxygen to underwater closed space

Table 4.1 Condition of hemoglobin solution

Hemoglobin concentration (mol/m ³)	5.43
pH	6.9
Ratio of IHP to Hemoglobin (mol:mol)	5:1
Density (kg/dm ³)	1.08
Specific heat capacity	2.88

4.2.2 Estimation of oxygen uptake and oxygen release rates

Oxygen transfer rate from water to the oxygen carrier solution and oxygen release rate from the oxygen carrier solution to air were estimated using an enhancement factor of the oxygen carrier solution. The enhancement factor of the oxygen carrier solution is expressed by the following equations:

$$E_u = -0.0000262 p_c + 3.2053 \quad (4.1)$$

$$E_r = -0.0001015 p_c + 19.501 \quad (4.2)$$

where E_u and E_r are the enhancement factors of the oxygen carrier solution in oxygen uptake and oxygen release, respectively, and p_c (Pa) is the oxygen partial pressure of the oxygen carrier solution. Sarns 5796 (3M, Tokyo), a commercially available membrane oxygenator, was used as a gas exchanger. This hollow fiber module, which is named as Module C in chapter 3, shows high gas exchange performance. Table 4.2 shows the technical data on Sarns 5796. Mass transfer coefficient when pure water flowed inside and outside this module was obtained, and oxygen transfer rate accompanied by oxygenation was calculated with the enhancement factor.

Table 4.2 Technical data on Sarns 5796

Membrane material	Polypropylene
Membrane surface area (m ²)	1.1
Outside diameter of hollow fibers (μm)	380
Membrane thickness (μm)	50
Volume of hollow fiber bundles (dm ³)	0.241

In the oxygen uptake device, overall mass transfer resistance $1/K_u$ is expressed by the equation:

$$\frac{1}{K_u} = \frac{1}{k_w} + \frac{1}{k_M} + \frac{1}{k_C} \quad (4.3)$$

where $1/k_w$ is the mass transfer resistance through the seawater, $1/k_C$ is the mass transfer resistance through the oxygen carrier solution and $1/k_M$ is the membrane resistance. When a porous polypropylene membrane is used, the membrane resistance is negligibly small [9-14]. Thus, the overall mass transfer resistance can be approximated by the equation:

$$\frac{1}{K_u} = \frac{1}{k_w} + \frac{1}{k_C} = \frac{1}{k_w} + \frac{1}{E \cdot k_L} \quad (4.4)$$

where $1/k_L$ is the mass transfer resistance through the pure water used as an oxygen carrier solution. The overall mass transfer coefficient was obtained by equation (4.4). The oxygen uptake rate N_u (mol/s) was estimated by following equation:

$$N_u = K_u A \alpha \Delta p_{lm} \quad (4.5)$$

where A (m^2) is the membrane surface area, α ($\text{mol}/\text{m}^3 \text{ Pa}$) is the physical solubility of oxygen, and Δp_{lm} (Pa) is the logarithmic mean difference of oxygen partial pressure. In the oxygen release device, the overall mass transfer resistance $1/K_r$ is expressed by the equation:

$$\frac{1}{K_r} = \frac{1}{k_C} + \frac{1}{k_M} + \frac{1}{k_G} \quad (4.6)$$

where $1/k_G$ is the mass transfer resistance through the air. When the porous polypropylene membrane is used, the membrane resistance is negligibly small. Thus, the overall mass transfer resistance can be approximated by the equation:

$$\frac{1}{K_r} = \frac{1}{k_C} = \frac{1}{E \cdot k_L} \quad (4.7)$$

The overall mass transfer coefficient was obtained by equation (4.7). The oxygen release rate N_r (mol/s) was estimated by following equation:

$$N_r = K_r A \alpha \Delta p_{lm} \quad (4.8)$$

4.2.3 Estimation of required heat transfer rate

In this artificial gill, the oxygen affinity of the oxygen carrier solution was controlled by changing temperature. Cooling oxygen carrier solution requires no energy because the seawater can be used to cool the oxygen carrier solution, whereas heating of the oxygen carrier solution requires energy. The required heat transfer rate for heating the oxygen carrier solution was obtained by the equation:

$$q = Q_c C_p \rho_c \Delta T \quad (4.9)$$

where q (J/s) is the required heat transfer rate, Q_c (m³/s) is the flow rate of the oxygen carrier solution, C_p (J kg⁻¹ K⁻¹) is the specific heat capacity of the oxygen carrier solution, ρ_c (kg/m³) is the density of the oxygen carrier solution and ΔT (K) is the range of temperature swing.

4.3 Results and discussion

4.3.1 Changing oxygen affinity with temperature

Fig. 4.2 shows the oxygen partial pressure of the oxygen carrier solution after heating to 310 K. The oxygen partial pressure increased by heating. This is because the oxygen affinity of hemoglobin is decreased, and hemoglobin dissociates much of its oxygen into the oxygen carrier solution. An increase in difference of oxygen partial pressure between oxygen carrier solution and air caused enhanced oxygen release. In contrast, the oxygen partial pressure decreased by cooling. An increase in difference of oxygen partial pressure between seawater and oxygen carrier solution caused enhanced oxygen uptake. This new system enables us to effectively transfer oxygen from seawater of low partial pressure of oxygen to air of high partial pressure of oxygen.

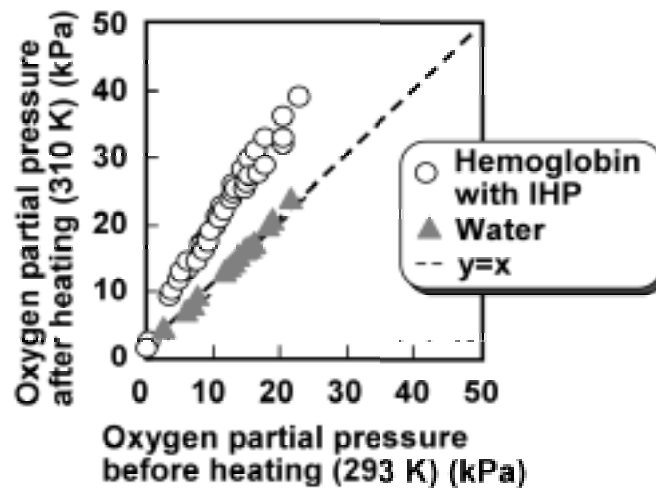


Fig. 4.2 Change in oxygen partial pressure in oxygen carrier solution with heating from 293 K to 310 K

4.3.2 Oxygen uptake and oxygen release rates

Fig. 4.3 shows overall mass transfer coefficient for oxygen of Sarns 5796 with water flowing inside and outside hollow fibers. Hollow fibers of Sarns 5796 are made of porous polypropylene. Thus, membrane resistance is negligibly small, and the overall mass transfer coefficient is equal to the fluid-side mass transfer coefficient. The oxygen uptake and oxygen release rates were estimated from mass transfer coefficient and enhancement factor. Fig.4.4 shows oxygen uptake rate as a function of water flow rate. The oxygen uptake rate was remarkably decreased at 12.0 kPa of seawater compared with at 20.0 kPa. This is because the difference of oxygen partial pressure between seawater and oxygen carrier solution was significantly decreased. The amount of dissolved oxygen in seawater supplying to the module was decreased, when oxygen partial pressure of seawater was low. These results indicate larger membrane surface area is required at a low oxygen partial pressure in seawater. Fig.4.5 shows the oxygen release rate as a function of oxygen carrier solution flow rate. The oxygen release rate increased with oxygen carrier solution flow rate. The oxygen release rate was much higher than the oxygen uptake rate. This demonstrates that the rate-determining step in this artificial gill system is located in the oxygen uptake device.

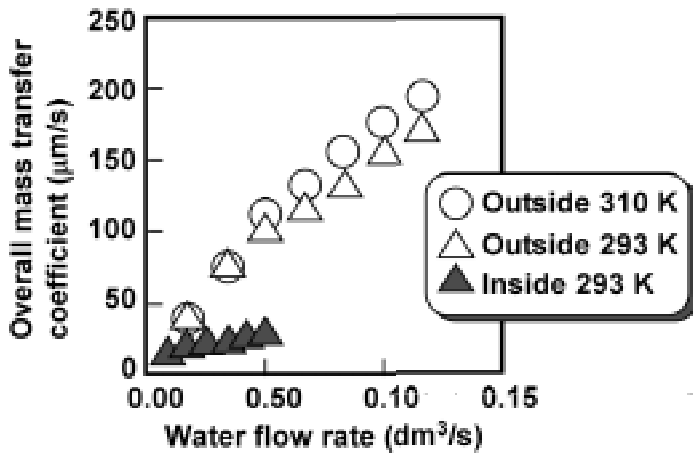


Fig. 4.3 Overall mass transfer coefficient for oxygen of hollow fiber module for water flowing inside and outside

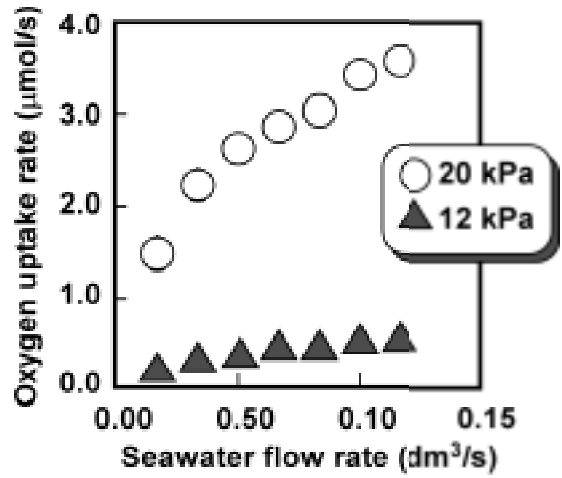


Fig. 4.4 Oxygen uptake rate as a function of water flow rate

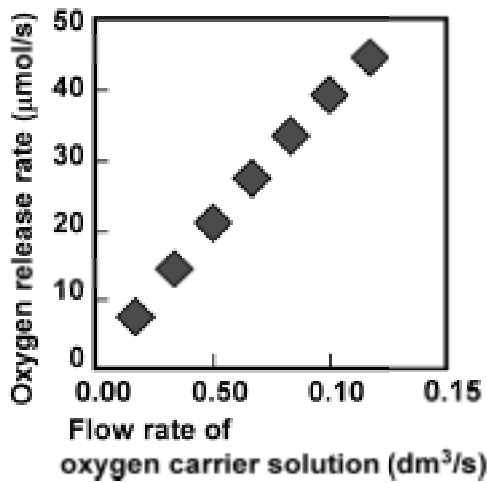


Fig. 4.5 Oxygen release rate as a function of flow rate of oxygen carrier solution

4.3.3 Designing artificial gill

Optimum operating conditions were evaluated by considering the required device volume and the device efficiency. The required membrane surface area, required device volume, the flow rates of oxygen carrier solution and heat transfer rate were determined. Fig. 4.6 shows the required membrane surface area and device volume, and Fig. 4.7 shows required seawater flow rate, oxygen carrier solution flow rate and heat transfer rate. The condition A was ordinary condition – the oxygen partial pressure of seawater was 20 kPa. The conditions B and C were assumed to be in low partial pressure of oxygen (12.0 kPa.). The condition B was adjusted to reduce the device volume, and the condition C was adjusted to reduce the seawater flow rate. Table 4.3 shows the operating conditions of each condition. The required membrane surface areas for oxygen uptake were markedly higher than that for oxygen release. Total device volume was larger when the oxygen partial pressure of seawater decreased for A, B and C. The required water flow rate, oxygen carrier solution flow rate and heat transfer rate of conditions B and C were higher than those of A. This demonstrates that the artificial gill requires much energy at lower oxygen partial pressures of seawater. The condition B requires higher flow rate of seawater, and the condition C requires larger device volume. When artificial gill is used for a submerged vessel, reducing energy for operating is more important than reducing device volume. Therefore, the condition C is suitable for use of plant-type artificial gill at lower partial pressures of oxygen.

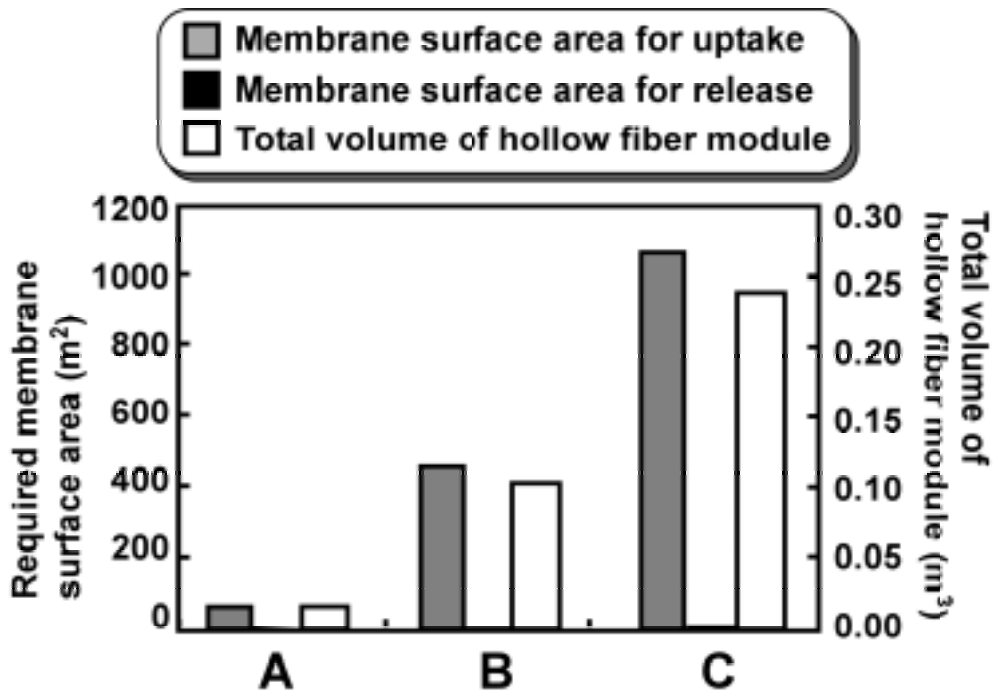


Fig.4.6 Required membrane surface area and total device volume

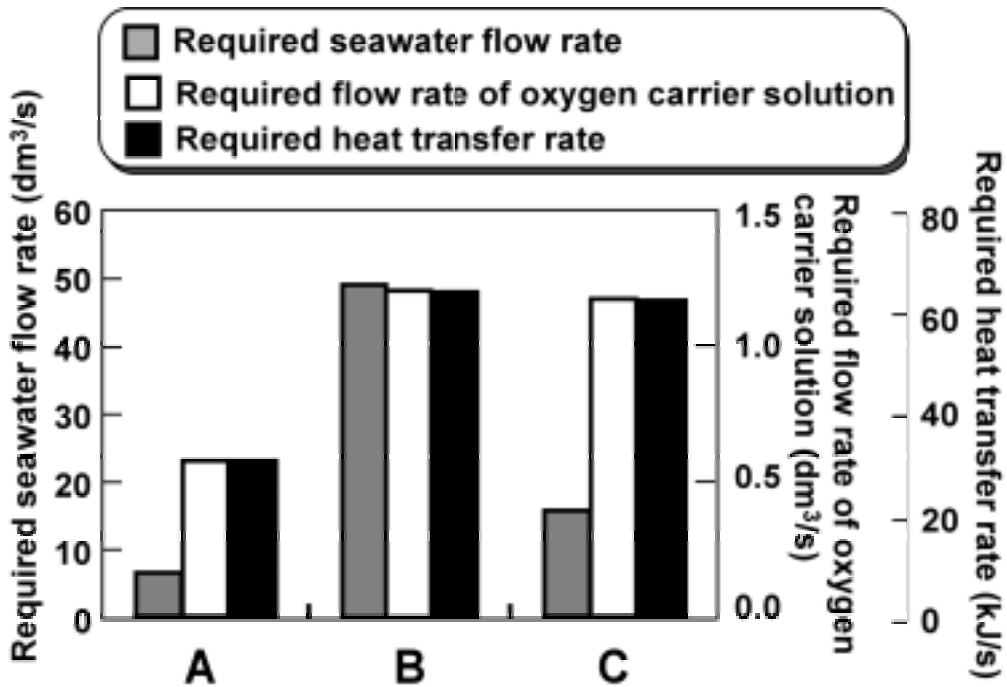


Fig.4.7 Required flow rate of seawater, oxygen carrier solution and heat transfer rate

Chapter 4

Table 4.3 Operating condition for artificial gill: (A) ordinary condition; (B) low oxygen partial pressure in seawater, minimum device volume; (c) low oxygen partial pressure in seawater, minimum flow rate

	A	B	C
Oxygen partial pressure in seawater (kPa)	20.0	12.0	12.0
Flow rate per module (dm ³ /s)			
Seawater	0.1000	0.1167	0.0167
Carrier in oxygen uptake	0.0083	0.0083	0.0083
Carrier in oxygen release	0.0833	0.1000	0.08333
Expired air	0.0417	0.0500	0.0417
Inlet oxygen partial pressure of oxygen carrier solution (kPa)			
In oxygen uptake	10.8	10.5	10.5
In oxygen release	22.6	21.3	21.3
Number of module connect			
Oxygen uptake			
In series	-	3	7
In parallel	70	142	140
Oxygen release			
In parallel	7	12	14

4.4 Conclusions

A plant-type artificial gill using hemoglobin solution was designed for supplying oxygen to underwater closed spaces such as submerged vessel, seabed-factory, and seabed city. The oxygen affinity of oxygen carrier solution was changed with temperature, and the oxygen partial pressure in the closed spaces was maintained to be sufficient oxygen partial pressure for human respiration (20.0 kPa). The oxygen uptake rate from water to oxygen carrier solution significantly decreased with oxygen partial pressure in seawater. The oxygen release rate was larger than the oxygen uptake rate. This result demonstrates that the rate-determining step is located in an oxygen uptake device. Optimum operating conditions were determined from oxygen uptake and release rates. Required membrane surface area and water flow rate are dependent on the oxygen partial pressure in seawater. Thus, additional membrane surface area is prepared for a decrease of oxygen partial pressure in seawater.

List of symbols

C	Specific heat capacity	(J kg ⁻¹ K ⁻¹)
E	Enhancement factor	(-)
k	Film mass transfer coefficient	(m/s)
K	Overall mass transfer coefficient	(m/s)
N	Oxygen transfer rate	(mol/s)
p	Oxygen partial pressure	(Pa)
Q	Flow rate	(m ³ /s)
ΔT	Range of temperature swing	(K)
ρ	Density	(kg/ m ³)

Subscripts

C	Oxygen carrier solution
G	Expired air
L	Pure water in place of an oxygen carrier solution
M	Membrane
r	Release
u	Uptake
W	Seawater

References

- 1) A.W. Ayres, Gill-type underwater breathing equipment and methods for reoxygenating exhaled breath, *US Patent*, 3,228,394, 1966
- 2) B.R. Bodell, Artificial gill, *Am. J. Med. Electron.*, 4 (1965) 170-171
- 3) B.R. Bodell, An artificial gill, *Surgical Forum*, 16 (1965) 173-175
- 4) C.V. Paganelli, N. Bateman, H. Rahn, Artificial gills for gas exchange in water, *Underwater Physiology*, C.J. Lambertsen, ed., Williams and Wilkins, Baltimore, 450 (1967)
- 5) M.C. Yang, E.L. Cussler, Artificial gills, *J. Membr. Sci.* 42 (1989) 273-284
- 6) N. Matsuda, K. Sakai, Technical evaluation of oxygen transfer rates of fish gills and artificial gills, *ASAIO J.*, 45 (1999) 293-298
- 7) K. Mizoguchi, Y. Suda, Y. Tanaka, T. Shimizu, A. Yamauchi, H. Ichijo, S. Ohnishi, Research on new types of artificial gill: I. Survey and analysis on R&D of artificial gill, *Bull. Res. Inst. Polymers and Textiles*, 154 (1987) 1-7
- 8) G. Nozawa, Atarashii Kaiyoukagaku, Seizandou Syoten, Tokyo (1990) pp.89-92
- 9) T.K. Kolobow, M. Borelli, R. Spatola, Artificial lung (oxygenators), *Artif. Organs*, 10 (1986) 370-377
- 10) M.E. Voorhees, B.F. Brian, Blood-gas exchange devices, *Int. Anesthesiol. Clin.*, 34 (2), (1996) 29-45
- 11) P.M. Galletti, Cardiopulmonary Bypass: A Historical Perspective. *Artif. Organs*, 17 (1993) 675-686
- 12) F. Yoshida, Prediction of oxygen transfer performance of blood oxygenators. *Artif. Organs Today*, 2 (1993):237-252
- 13) H. Nakanishi, Y. Nishitani, K. Kuwana, Y. Aoki, S. Osaki, Hu C., Development of new oxygenator with cyclosiloxane coated polypropylene

Chapter 4

hollow fibers, *Jpn. J. Artif. Organs*, 25 (1996) 329-332

- 14) Y. Niimi, K. Ueyama, K. Yamaji, S. Yamane, E. Tayama, A. Sueoka, K. Kuwana, K. Tahara, Y. Nose, Effect of ultrathin silicone coating of porous membrane on gas transfer and hemolytic performance, *Artif. Organs*, 21 (10) 1082-1086